

LETTER

Open Access



# A 3D-printed pneumatic dispenser with monitoring droplet ejection

Dong Kwan Kang<sup>1</sup>, Jeong Woo Park<sup>2</sup> and Sangmin Lee<sup>2\*</sup> 

## Abstract

In this study, a pneumatic dispenser driven by a flexible membrane with a capacitive-type sensor using an SLA-type 3D printer was fabricated. It was confirmed that a single droplet in the range of approximately 400–450 nL could be ejected from the current processed 200- $\mu$ m-diameter nozzle. The deformation varied according to the magnitude and time of the positive pressure applied to the membrane sensor. In addition, the signals of the normal dispensing and abnormal states, in which the solution was not ejected when the inlet pressure was removed, were measured and compared. The base capacitance-to-digital converter (CDC) value decreased when the inlet pressure was removed. Thus, it was able to confirm the feasibility of monitoring the normal and abnormal ejection status of the pneumatic dispenser.

**Keywords:** Pneumatic, Dispenser, Membrane sensor, Monitoring

## Introduction

Inkjet printing, based on drop-on-demand, is a non-contact printing technology that can deliver a liquid material, in the form of micro-droplets, precisely to a desired location [1]. Thus, the amount of material consumed is reduced, various types of substrates can be patterned. Therefore, this technology is being employed in various industrial fields [2, 3].

In the field of printed electronics, various functional materials such as electronic devices, including color filters and transistors of displays, are used in conjunction with electrode printing for manufacturing using inkjet technology [4]. In tissue engineering, bio-ink is widely employed as a bioprinting system for artificial tissues or organs [5].

Currently, for packaging various electronic products in the manufacturing industry, a jetting valve-type printing system is used to apply a high-viscosity material, such as an epoxy molding compound (EMC) or adhesive, to

an accurate location. Using the jetting valve method, a highly-pressurized high-viscosity solution is delivered, and the solution is dispensed while the high-speed valve included in the nozzle opens and closes. Materials used in packaging mainly contain polymer particles, therefore, nozzle clogging problems can easily occur, requiring considerably maintenance cost and effort, such as periodic cleaning [6].

Various monitoring methods for the dispensing state have been developed to prevent printing nozzle failure and efficient maintenance cycle confirmation. For example, a method for monitoring the ejection process by periodic image analysis using a high-speed camera [7] or monitoring the movement of ejected droplets using millimeter waves in real-time has been studied [8]. Alternatively, a method for monitoring the failure of a multi-nozzle printer by applying a self-sensing method to a piezo-type inkjet printer has been studied [9].

In this study, we introduced a pneumatic dispenser [10–12] that can monitor the droplet ejection status in real-time using a capacitive-type sensor embedded on a flexible membrane using pneumatic pressure deformation. The difference between the membrane deformation under normal and abnormal operating conditions was

\*Correspondence: thinking@deu.ac.kr

<sup>2</sup> Division of Mechanical, Automotive and Robot Component Engineering, Dong-Eui University, Busan 47340, South Korea  
Full list of author information is available at the end of the article

analyzed using the sensing signal of the embedded sensor, and the droplet ejection status was monitored in real-time. In addition, all parts of the dispenser were designed and fabricated at a size suitable for printing using a stereolithography (SLA)-type 3D printer. The dispensing and sensing performance of the fabricated dispenser was verified. The difference between the normal and abnormal sensing signals for dispensing status monitoring was analyzed.

## Experiments and method

### Design and fabrication of pneumatic dispenser

The configuration of the pneumatic dispenser capable of monitoring droplet ejection is shown in Fig. 1. The dispenser includes an actuation part that controls the pneumatic pressure using a solenoid valve, a membrane

sensor part that includes a membrane deformed by pneumatic pressure to eject a liquid solution, a capacitive-type sensor for measuring deformation, and solution inlet and outlet nozzles composed of microchannels. The actuation and microchannel parts were manufactured using an SLA-type 3D printer (Form2, FormLab). A rigid resin (Rigid 10 K Resin V1) was used for the microchannels, and a clear resin (Standard Clear resin V4) was used for the actuation part. The membrane sensor was manufactured using polydimethylsiloxane (PDMS) and consisted of a membrane and supporting block. The membrane was deformed with pneumatic pressure to eject droplets, and silver nanowire (AgNW) electrodes were patterned on the membrane surface to measure deformation.

The pneumatic dispenser fabrication process is illustrated in Fig. 2. First, after the designed (a-1)

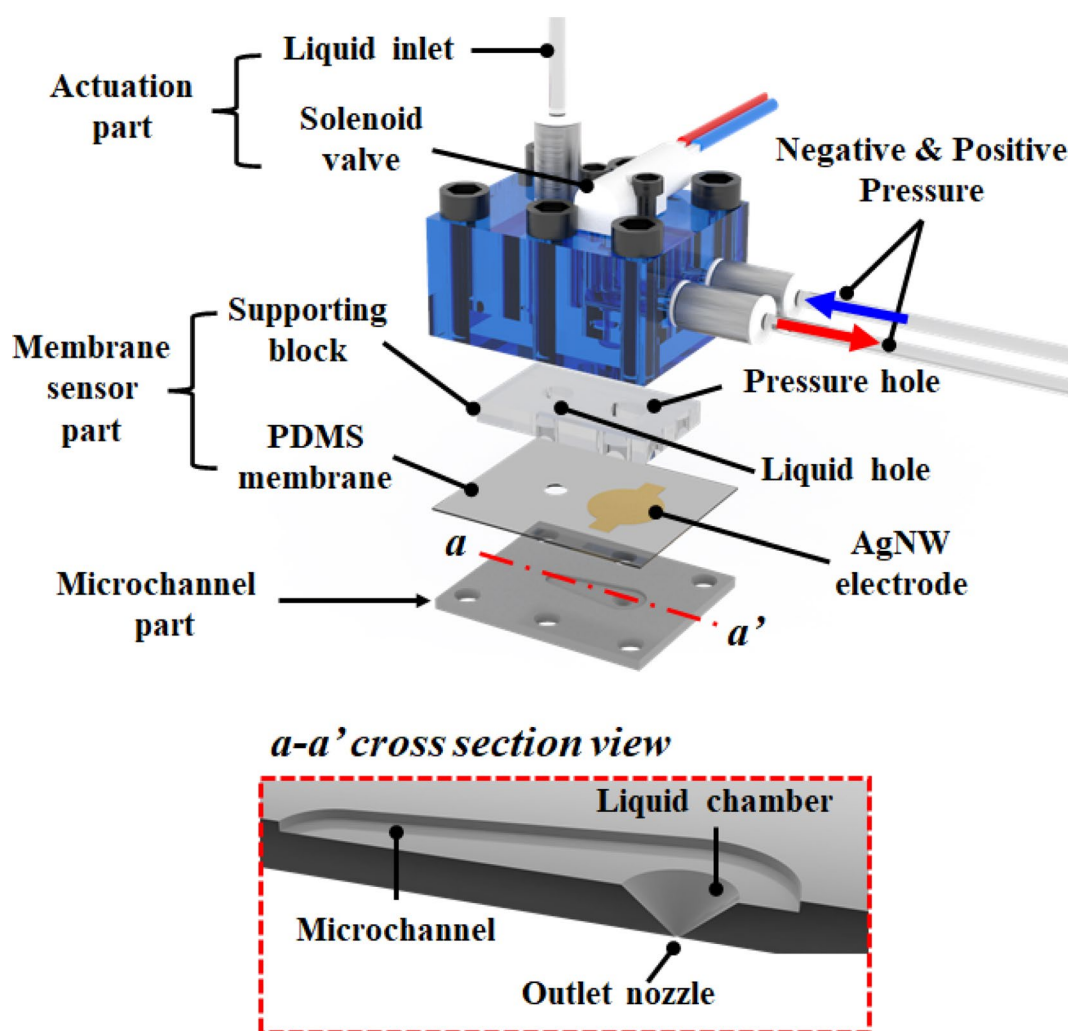


**Fig. 1** Schematic of the configuration of a pneumatic dispenser capable of monitoring droplet ejection

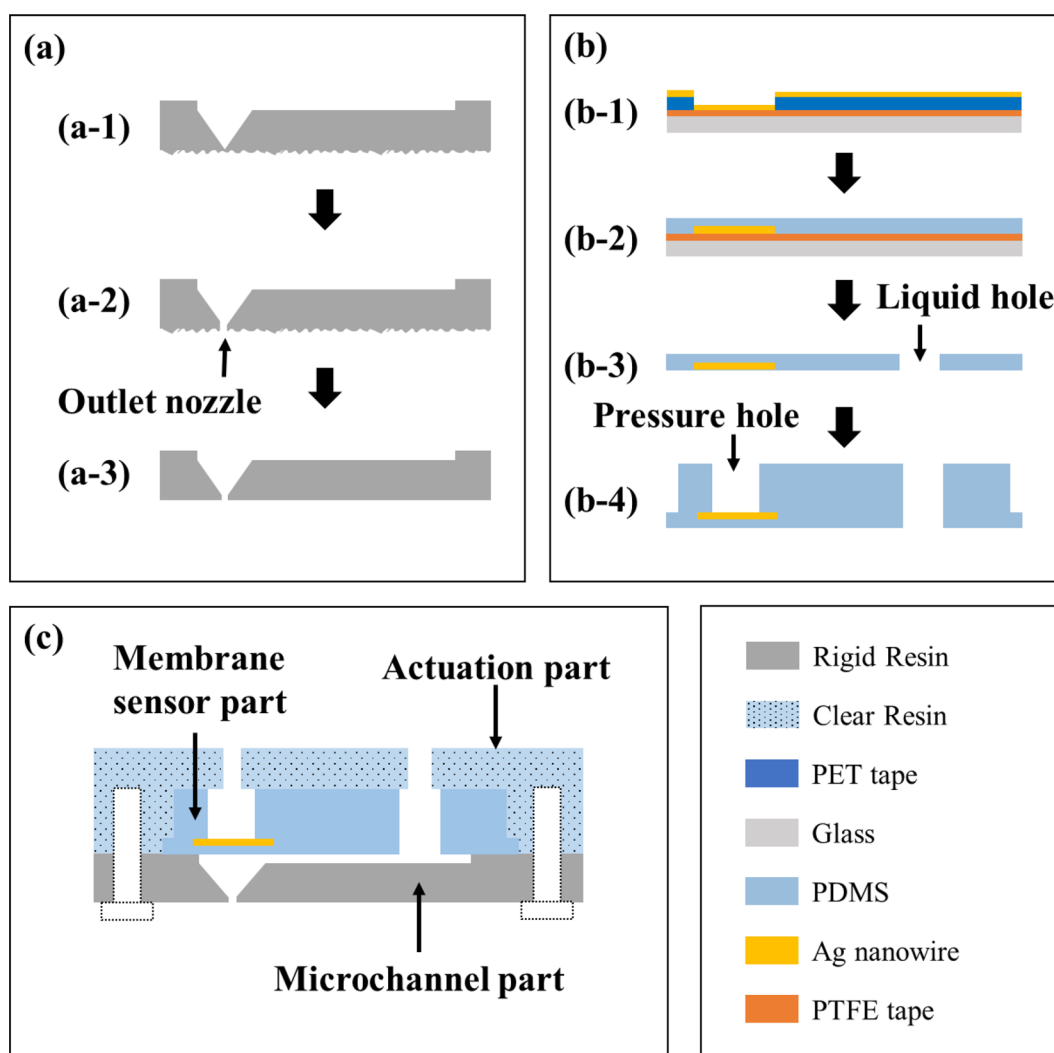


**Fig. 2** Fabrication process of a pneumatic dispenser; **a** microchannel, **b** membrane sensor, and **c** assembled dispenser

microchannel was printed with a 3D printer, an outlet nozzle with a 200  $\mu\text{m}$  diameter was manufactured through drilling. Subsequently, the surface around the nozzle was smoothed using sandpaper. Next, a Teflon (AF-1600, 0.05%) dip-coating was applied for a hydrophobic coating around the nozzle.

For membrane fabrication with AgNW electrodes, a substrate with polytetrafluoroethylene (PTFE) tape attached to a glass slide was prepared. The AgNW solution (Flexiowire 2020, Flexio Co., Ltd.) was then patterned using a spray gun (b-1). After mixing the curing agent at a weight ratio of 10:1 on the patterned electrode, a PDMS solution (Sylgard 184 Silicone Elastomer, Dow Corning) membrane was poured and spin-coated at 500 rpm for 30 s (b-2). The cured PDMS

membrane was slowly peeled off in an oven at 70  $^{\circ}\text{C}$  for 4 h, and a liquid hole was formed by punching (b-3). The thickness of the membrane was  $297 \pm 3.77 \mu\text{m}$ .

The dispenser was designed to have no bonding between the PDMS membrane, microchannel, and actuation. A supporting block was designed to prevent leakage of the pneumatic pressure applied to the membrane and ejected solution. A 3 mm thick PDMS block was made of the same material as the membrane, and pressure and liquid holes were drilled for the in- and outlet of the pneumatic pressure and solution. Subsequently, the PDMS membrane and supporting block were completed by bonding the two surfaces after the air plasma treatment (45 W, 30 s) (b-4). The dispenser was completed by fastening/assembling the manufactured parts using bolts (Fig. 2c).

### Operating and sensing droplet ejection

A schematic of the operating principle of the dispenser is shown in Fig. 3a, b. Normally, a negative pressure is applied to the membrane through the solenoid valve, which causes the membrane to deform in the opposite direction of the nozzle. The liquid solution delivered at a constant inlet pressure fills the liquid chamber inside the dispenser. When the solenoid valve is turned on by applying an electrical signal for the programmed time, a positive pressure is applied to the membrane. The positive pressure causes the membrane to deform in the nozzle direction and to push the liquid solution. However, a certain amount of the liquid solution is dispensed out of the nozzle. The signal for precise control of the solenoid valve is shown in Fig. 3c.

When the dispenser is driven, membrane deformation is sensed by measuring the real-time change in capacitance between the AgNW electrode patterned on the membrane surface and the ground electrode made from Cu tape inside the pressure hole. If the membrane deforms in the opposite direction of the negatively pressurized nozzle, it gets closer to the ground electrode, and the capacitance increases. Conversely, the capacitance decreases if it is deformed in the positively pressurized nozzle direction. The change in capacitance was measured using an AD7147 programmable capacitance-to-digital converter (CDC) and collected as a CDC counter (CDC output) [13]. The collected CDC counter was transmitted to the MCU (Cortex-M3, ARM) through I<sup>2</sup>C (inter-integrated circuit) communication. The data

were transmitted to the PC through serial communication and recorded at a sampling rate of approximately 1 kHz. LabView<sup>TM</sup> software (National Instruments<sup>®</sup>) and a digital input/output (DIO) board were used for solenoid valve signal control and data collection.

Deionized water was used as the experimental solution. The ejection process and the volume and speed of the ejected droplets were recorded at a speed of 20,000 fps (frames per second) using a high-speed camera (FAST-CAM MiniAX, Photron), and the images were recorded using digital image processing in MATLAB<sup>®</sup>. The volume and velocity of the droplets were quantitatively measured.

## Results and discussion

### Sensing membrane deflection

To evaluate the membrane sensor performance, the capacitance change of the membrane sensor was measured at atmospheric pressure without a liquid solution. First, the sensor signal was measured while increasing the solenoid valve opening time (push time) from 8 to 200 ms, and the pressures (positive and negative pressure) applied to the membrane were fixed at 5 and -3 kPa, respectively (Fig. 4).

When positive pressure was applied during the push time, the CDC value decreased as the membrane moved away from the ground electrode. When negative pressure was applied to the membrane again during the pull time, the CDC value increased as the membrane

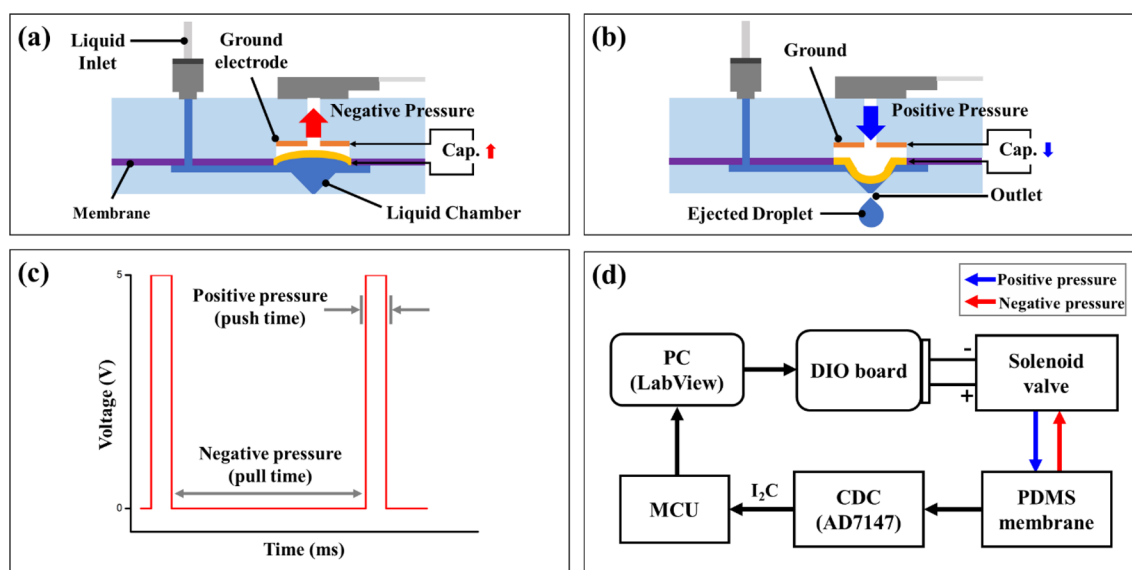


**Fig. 3** Schematics of dispensing mechanism and signal processing; membrane deformation and droplet ejection process by **a** positive, **b** negative pressure, **c** a graph of the solenoid valve control signal, and **d** a diagram for measurement of control and sensor signals

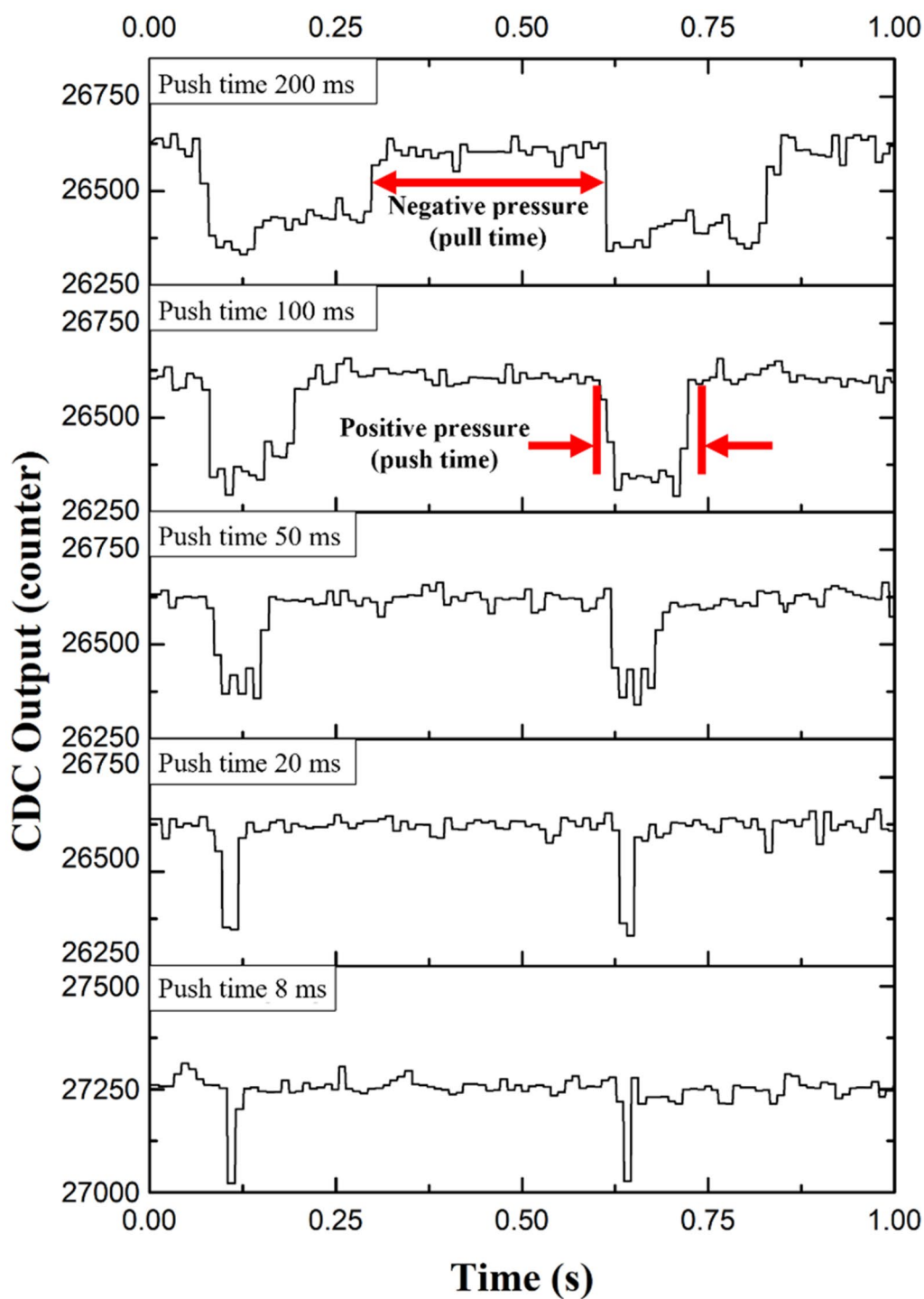


**Fig. 4** Results of measured membrane sensor signal by controlling the push time

approached the ground electrode. Based on the CDC value in a state where negative pressure was applied to the membrane, the CDC value reduced by deformation by positive pressure was approximately  $244 \pm 78$

counts, which was measured as a similar value in the push time control range.

In addition, as the push time input in the program increased, the CDC value decreased and the

maintenance time increased. However, for the delay time of the solenoid valve, there was a time error between the programming push time and the actual push time of the sensor signal, owing to the actual membrane deformation. Over the entire push time range, the time error was calculated in the range of 0.022 to 30 ms, and in the range of coefficient of variation (CV) from 3–21%.

The signal measuring result, due to deformation of the membrane, with increasing positive pressure is shown in

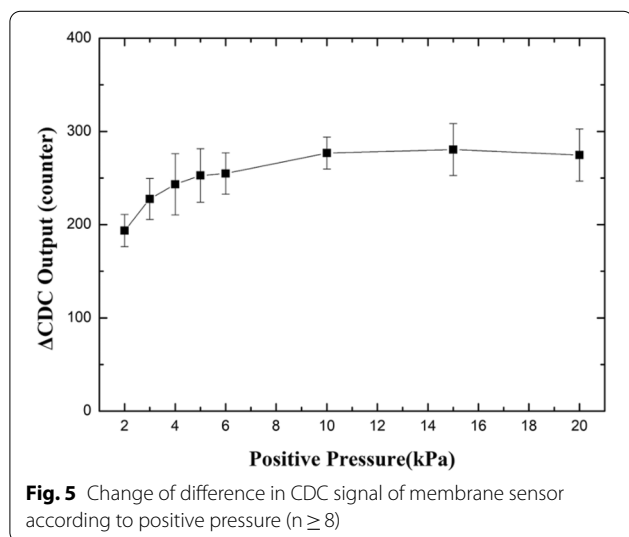
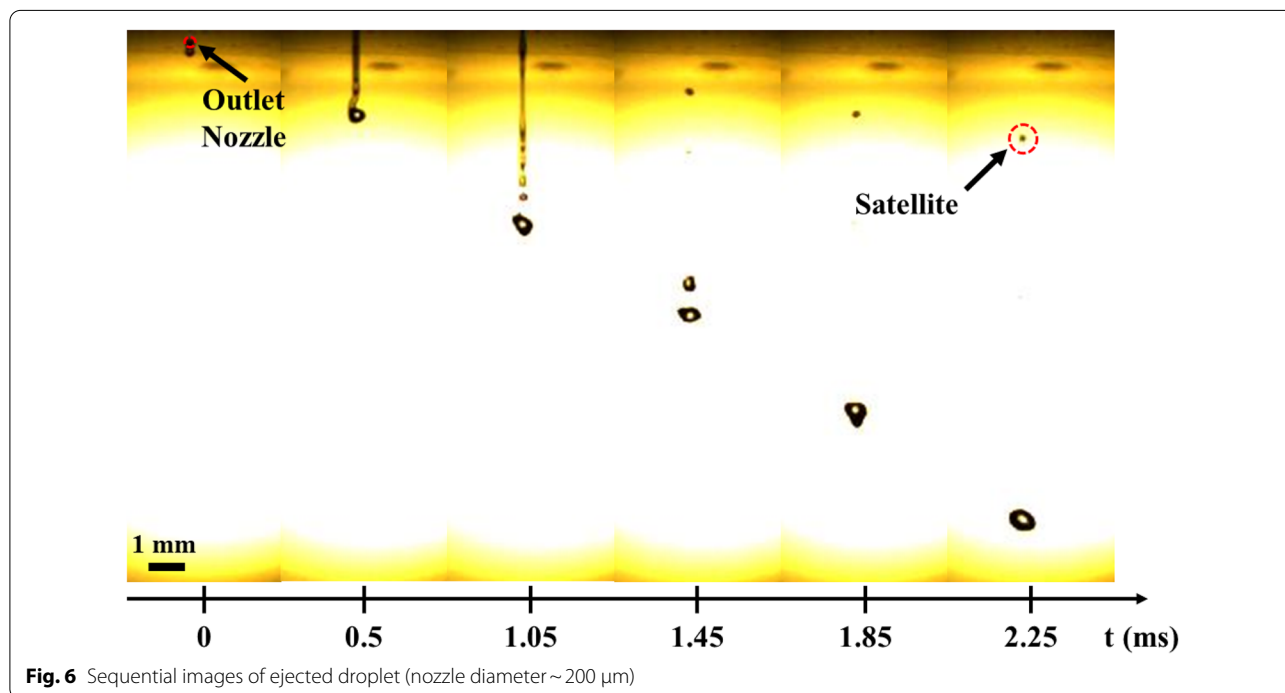


Fig. 5. The negative pressure and push time were fixed at  $-3$  kPa and 20 ms, respectively, and the measurement was repeated more than 10 times while increasing the positive pressure from 2 to 20 kPa. As the magnitude of the positive pressure increased, the magnitude of the signal increased. Above 10 kPa, the signal magnitude tended to saturate. In the air, the liquid chamber size limited the deformation of the membrane, and no further deformation occurred.

#### Dispensing a liquid droplet

The membrane was deformed when the liquid solution was supplied through the inlet hole at constant pressure (4.8 kPa), and a condition in which a single droplet of a constant volume was stably ejected was confirmed. Figure 6 shows a sequential image of the ejection process from an approximate 200- $\mu\text{m}$ -diameter nozzle. The positive and negative pressures applied to the membrane were 5 and  $-3$  kPa, respectively, and the push time was 8 ms. It was confirmed that a single droplet was stably ejected through the nozzle. In the initial liquid jet ejected through the nozzle, the liquid in the tail end that did not merge with the main droplet, instead remained to form small droplets, called satellite droplets. In addition, the satellite droplet phenomenon becomes more pronounced as the surface tension of the liquid increases [14]. Most of the generated satellite droplets merged with the main droplet during the droplet fall process. However, in the case when a satellite droplet was irregularly formed or





did not merge with the main droplet, the printing resolution was reduced. The satellite droplet shown in Fig. 6 merged after the falling, and the droplets observed just before the collision on a solid substrate were identified as a single droplet.

Figure 7 shows variation in volume and velocity of the ejected droplet with varying positive pressure, under the stable ejection of a single droplet. The positive pressure increased from 2 to 5 kPa, while the other conditions remained constant. The ejected volume increased to 395–445 nL, and the measured velocity was 11–15 m/s.

### Monitoring droplet ejection

To monitor droplet ejection from the dispenser using a membrane sensor, the sensor signal under abnormal and normal ejection conditions were compared. Figure 8a shows the measured CDC values in the normal ejection condition under a positive pressure of 5 kPa, negative pressure of -3 kPa, push time of 8 ms, pull time of 500 ms, and inlet pressure of 4.8 kPa to supply the liquid solution. When positive pressure was applied, the membrane

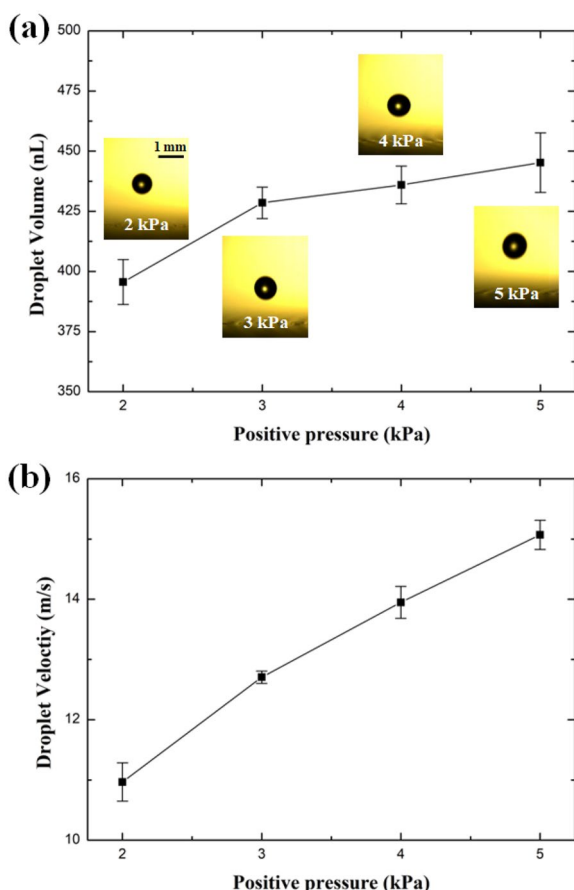


**Fig. 7** Measurement results of **a** droplet volume and **b** velocity of ejected droplet according to positive pressure ( $n = 10$ )

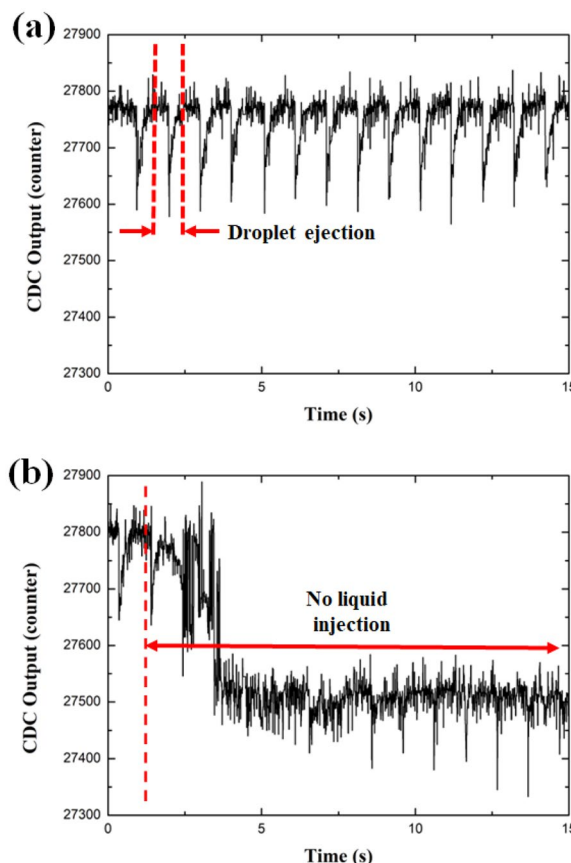


**Fig. 8** Measured sensor signal under **a** the normal and **b** abnormal ejecting conditions

deformed in the nozzle direction and pushed the liquid solution out of the nozzle. Simultaneously, the membrane moved away from the ground electrode, and the CDC value decreased by  $288 \pm 19$  counts. As negative pressure was applied, the membrane deformed in the opposite direction away from the nozzle. As it approached the ground electrode, the CDC value increased to the previous level.

During the normal ejection process, when the inlet pressure for the liquid solution supply was removed, regardless of whether the positive and negative pressures deform the membrane, the solution could not be supplied to the solution chamber, and the droplet could no longer be ejected. The CDC values of the sensor measured after the removal of the inlet pressure are shown in Fig. 8b. Instead, the base CDC value in the pull time decreased by approximately 300 counts compared to the normal state. A decrease in the CDC value indicates an increase in the distance between the membrane and the ground electrode. In the normal ejection state, the membrane is deformed toward the ground electrode by the

inlet pressure, and when the inlet pressure is removed, the distance from the ground electrode increases.

## Conclusion

This study evaluated a fabricated pneumatic dispenser driven by a flexible membrane with a capacitive-type sensor using an SLA-type 3D printer. It was confirmed that a single droplet in the range of 400–450 nL could be ejected from the currently processed 200- $\mu$ m-diameter nozzle. In addition, the deformation varied with the magnitude and duration of the positive pressure applied to the membrane through the sensor.

In addition, the signals of the normal and abnormal states, in which the solution was not ejected upon the removal of the inlet pressure, were measured and compared. The base CDC value decreased when the inlet pressure was removed. Thus, it was able to confirm the feasibility of monitoring the normal and abnormal ejection status of the pneumatic dispenser.

The future researches will aim to improve the stability of the membrane sensor with flexible electrode and the precision of the measurement circuit and system. After confirming the stable output signal, we plan to analyze the sensor's response to various error conditions (e.g., nozzle wetting and low positive pressure) and study signal changes according to the physical properties of various solutions.

## Abbreviations

AgNW: Silver Nanowire; PTFE: Polytetrafluoroethylene.

## Acknowledgments

Not applicable.

## Author contributions

DKK carried out the experiments and drafted the manuscript. JWP analyzed the experimental result. SL drafted, read, and approved the final manuscript. All authors read and approved the final manuscript.

## Funding

This work was supported by the National Research Foundation of Korea (NRF) grant funded by the Korea government (MSIT) (No. 2020R1F1A1050735).

## Availability of data and materials

The datasets and a movie supporting the conclusions of this article are included within the article.

## Declarations

## Competing interests

The authors declare that they have no competing interests.

## Author details

<sup>1</sup>The Research Institute of Artificial Intelligence Robots, Dong-Eui University, Busan 47340, South Korea. <sup>2</sup>Division of Mechanical, Automotive and Robot Component Engineering, Dong-Eui University, Busan 47340, South Korea.

Received: 25 August 2022 Accepted: 12 October 2022

Published online: 31 October 2022

## References

- da Costa TH, Choi JW (2020) Low-cost and customizable inkjet printing for microelectrodes fabrication. *Micro Nano Syst Lett* 8(2):1–6. <https://doi.org/10.1186/s40486-020-0104-7>
- Chiolerio A, Virga A, Pandolf P, Martino P, Rivolo P, Geobaldo F, Giorgis F (2012) Direct patterning of silver particles on porous silicon by inkjet printing of a silver salt via in-situ reduction. *Micro Nano Syst Lett* 7(502):1–7
- Andò B, Baglio S (2013) All-inkjet printed strain sensors. *IEEE Sens J* 13(12):4874–4879. <https://doi.org/10.1109/JSEN.2013.2276271>
- Khan Y, Thielens A, Muin S, Ting J, Baumbauer C, Arias AC (2020) A new frontier of printed electronics: flexible hybrid electronics. *Adv Mater* 32(15):e1905279. <https://doi.org/10.1002/adma.201905279>
- Li X, Liu B, Pei B, Chen J, Zhou D, Peng J, Zhang X, Jia W, Xu T (2020) Inkjet Bioprinting of biomaterials. *Chem Rev* 120(19):10793–10833. <https://doi.org/10.1021/acs.chemrev.0c00008>
- Li Y, Dahhan O, Filipe CDM, Brennan JD, Pelton RH (2019) Deposited nanoparticles can promote air clogging of piezoelectric inkjet printhead nozzles. *Langmuir* 35(16):5517–5524. <https://doi.org/10.1021/acs.langmuir.8b04335>
- Wang F, Wang Y, Bao W, Zhang H, Li J, Wang Z (2020) Controlling Ejection State of a Pneumatic micro-droplet Generator through machine vision methods. *Int J Precis Eng Manuf* 21(4):633–640. <https://doi.org/10.1007/s12541-019-00295-7>
- Chang T, Mukherjee S, Watkins NN, Benavidez E, Gilmore AM, Pascall AJ, Stobbe DM (2021) Millimeter-wave electromagnetic monitoring for liquid metal droplet-on-demand printing. *J Appl Phys* 130(14):144502. <https://doi.org/10.1063/5.0065989>
- Wang L, Wang K, Hu H, Luo Y, Chen L, Chen S, Lu B (2020) Inkjet jet failures detection and droplets speed monitoring using piezo self-sensing. *Sens Actuators A* 313:112178. <https://doi.org/10.1016/j.sna.2020.112178>
- Choi IH, Kim J (2016) A pneumatically driven inkjet printing system for highly viscous microdroplet formation. *Micro Nano Syst Lett* 4(1):1–7. <https://doi.org/10.1186/s40486-016-0030-x>
- Lee S, Kim H, Kim J (2017) Feasibility study of a biocompatible pneumatic dispensing system using mouse 3T3-J2 fibroblasts. *Micro Nano Syst Lett* 5(1):1–7. <https://doi.org/10.1186/s40486-017-0061-y>
- Lee S, Choi IH, Kim YK, Kim J (2014) Velocity control of nanoliter droplets using a pneumatic dispensing system. *Micro Nano Syst Lett* 2(1):1–7. <https://doi.org/10.1186/s40486-014-0005-8>
- Won DJ, Huh M, Lee S, Park U, Yoo D, Kim J (2020) Capacitive-type two-axis accelerometer with liquid-type proof mass. *Adv Electron Mater* 6(6):1901265. <https://doi.org/10.1002/aelm.201901265>
- Jang D, Kim D, Moon J (2009) Influence of fluid physical properties on inkjet printability. *Langmuir* 25:2629–2635

## Publisher's Note

Springer Nature remains neutral with regard to jurisdictional claims in published maps and institutional affiliations.

**Submit your manuscript to a SpringerOpen<sup>®</sup> journal and benefit from:**

- Convenient online submission
- Rigorous peer review
- Open access: articles freely available online
- High visibility within the field
- Retaining the copyright to your article

Submit your next manuscript at ► [springeropen.com](https://www.springeropen.com)